Simulation of x-ray absorption near-edge spectra and x-ray fluorescence spectra of optically excited molecules

R. K. Pandey and Shaul Mukamel[a)]
Department of Chemistry, University of California, Irvine, California 92697-2025

(Received 18 November 2005; accepted 17 January 2006; published online 2 March 2006)

The x-ray absorption near-edge spectra (XANES) and fluorescence spectra of molecules in the ground state and optically excited states are computed using time-dependent density functional theory and time-dependent Hartree-Fock theory. The calculated XANES spectra of optically excited methanol, benzonitrile, hydrogen sulphide, and titanium tetrachloride and the fluorescence spectra of optically excited methanol can be used to simulate ultrafast optical pump/x-ray probe experiments. © *2006 American Institute of Physics*. [DOI: 10.1063/1.2173243]

I. INTRODUCTION

Resonant x-ray spectroscopy is widely used for the characterization of atoms, molecules, and materials.[1–5] X-ray signals can access the entire electronic manifold of atoms and molecules and have different selection rules than optical spectroscopy. X-ray absorption near-edge spectroscopy (XANES) can measure variations in electronic structure due to changes in atomic positions (geometry) and charge distributions of transient species during and after photoexcitation.[6,7] This region of the x-ray absorption spectra of up to ~20 eV above the absorption threshold gives information about the unoccupied density of states of a molecule in the vicinity of the absorbing atom. These states are important for the formation of chemical bonds. X-ray fluorescence spectra are sensitive to the electronic structure (occupied density of states) of molecules in the vicinity of an atom.[8–10] There have been rapid advances in the studies of x-ray absorption and emission spectroscopies over the past decade.[2,3] Femtosecond to attosecond sources can be used to study elementary electronic and vibrational processes in molecules, liquids, and crystals[4,5] and enable the real time probing of optically induced electron motions and chemical processes.

The sum over states[6,11,12] (SOS) and the transition potential[13–16] (TP) methods are commonly used for computing XANES spectra. The SOS method requires calculations of two different sets of orbitals (ground state and core excited state) and allows the employment of any level of quantum chemistry calculations of electronically excited states. The TP method uses a reference system with partially filled orbitals. Only one reference set of orbitals is calculated, and systems with different numbers of core holes are represented by varying the occupation numbers. This technique is computationally less expensive and was successfully applied to small molecules.[13–16]

In this paper we compute XANES and fluorescence spectra of molecules using the SOS protocol previously applied to ruthenium tris-2,2′-bipyridine complex.[6] All electronic structure calculations are performed within density functional theory using the correlation functional (B3LYP) or the Hartree-Fock (HF) approximation. Both the ground state and the lowest core excited state [$Z+1$ approximation, the ground state of $Z+1$ and $N+1$ systems (N is the number of electrons and Z is the nuclear charge of the absorbing atom)] are calculated. Valence excited states are obtained using time-dependent density functional theory (TDDFT) or time-dependent Hartree-Fock (TDHF) theory.[6] The computed ground state XANES spectra of H_2O, CH_3OH, C_6H_5CN H_2S, and $TiCl_4$ are compared with the experiment. We predict the XANES spectra of CH_3OH, C_6H_5CN, H_2S, and $TiCl_4$ in their low lying valence excited states. We further calculate the x-ray fluorescence spectra of H_2O, CH_3OH, H_2S, and $TiCl_4$ in their ground states and the O K-fluorescence spectra of CH_3OH in its low lying excited states.

II. METHODOLOGY

A. XANES

We start with the deep core Hamiltonian of Mahan[17] and Nozieres and DeDominicis.[18]

$$H=\sum_{lm}^{\mathrm{val}}\epsilon_{lm}c_l^\dagger c_m+\sum_{g}^{\mathrm{core}}\epsilon_g c_g^\dagger c_g+\sum_{jklm}^{\mathrm{val}}V_{jklm}c_j^\dagger c_k^\dagger c_m c_l+\sum_{g}^{\mathrm{core}}\sum_{lm}^{\mathrm{val}}U_{lm,g}c_l^\dagger c_m c_g c_g^\dagger, \tag{1}$$

where $c_l^\dagger(c_l)$ is the creation (annihilation) operator for an electron in orbital l. We use a.u. ($m_e=\hbar=e=1$) and assume that the core electrons with energies ϵ_g are noninteracting.

$$\epsilon_{lm}=\left\langle l\left|-\frac{\hat{\mathbf{p}}^2}{2}+\sum_{a}^{\mathrm{nucl}}\frac{Z_a}{|\hat{\mathbf{r}}-\mathbf{r}_a|}\right|m\right\rangle+\sum_{g}^{\mathrm{core}}[V_{lgmg}-V_{lggm}]c_g^\dagger c_g \tag{2}$$

is the one electron Hamiltonian, which includes the kinetic energy, the Coulomb attraction to the nuclei, the Coulomb,

a)Electronic mail: smukamel@uci.edu

and the exchange interaction with all core electrons. The valence electron-electron interactions are given by

$$V_{jklm} = \int d\mathbf{x}_1 d\mathbf{x}_2 \langle j|\mathbf{x}_1\rangle\langle k|\mathbf{x}_2\rangle \frac{1}{|\mathbf{r}_1 - \mathbf{r}_2|}\langle \mathbf{x}_1|l\rangle\langle \mathbf{x}_2|m\rangle, \tag{3}$$

where $\mathbf{x}=(\mathbf{r},s)$ denotes both space and spin variables. Since the core hole is highly localized compared to the valence electron orbitals, it acts as a point charge for the valence electrons. We therefore take it into account using the $Z+1$ approximation, whereby the nuclear charge Z of the absorbing atom is increased by one. As a consequence, the fourth term in the Hamiltonian (core-valence interaction term) which includes both the Coulomb attraction and the exchange interaction between the electrons in valence orbitals l and m and the core hole in orbital g can be approximated as

$$U_{lm,g} = \left\langle l \left| \frac{1}{|\hat{\mathbf{r}} - \mathbf{r}_0|} \right| m \right\rangle, \tag{4}$$

where $\mathbf{r}_0$ is the position of the absorbing atom. The $Z+1$ approximation describes the valence excitation and ignores the deep-core excitation dynamics.

The absorption cross section of the x-ray photon with frequency ω and polarization λ is given by

$$\sigma_{\text{abs}}(\omega,\lambda) = \frac{4\pi^2}{\omega c}\sum_f |\langle \Psi_i|\mu^\lambda|\Psi_f\rangle|^2 \delta(\omega + E_i - E_f), \tag{5}$$

where $|\Psi_i\rangle$ ($|\Psi_f\rangle$) is the initial (final) electronic state with energy E_i (E_f). $|\Psi_i\rangle$ can be either the ground state or an optically excited state. The electronic dipole operator is

$$\mu^\lambda = \sum_{gj} \mu^\lambda_{gj} c_g c_j^\dagger, \tag{6}$$

where μ^λ_{gj} is the one electron dipole matrix element between the core orbital $|g\rangle$ and the unoccupied valence orbital $|j\rangle$,

$$\mu^\lambda_{gj} = \langle g|\boldsymbol{\lambda}\cdot\hat{\mathbf{p}}|j\rangle, \tag{7}$$

where $\boldsymbol{\lambda}$ is the unit vector along λ. Substitution of Eq. (6) into Eq. (5) gives

$$\sigma_{\text{abs}}(\omega,\lambda) = \frac{4\pi^2}{\omega c}\sum_{g,lm}\sum_f \mu^\lambda_{lg}\mu^\lambda_{gm}\langle \Psi_i|c_l c_g^\dagger|\Psi_f\rangle \times \langle \Psi_f|c_g c_m^\dagger|\Psi_i\rangle \delta(\omega - E_i - E_f). \tag{8}$$

The Hamiltonian [Eq. (1)] gives a separate eigenvalue problem for the core and valence electrons. Hence we can factorize the total wave function $|\Psi\rangle$ into a product of the fully correlated N electron valence wave function $|\Phi^N\rangle$ and the ground state core wave function $|G_0\rangle$: $|\Psi_i\rangle = |\Phi^N\rangle|G_0\rangle$ and $|\Psi_f\rangle = |\Phi'^{N+1}\rangle|G'_g\rangle$, where $|G'_g\rangle$ is the core wave function when the core orbital g is unoccupied and $|\Phi'^{N+1}\rangle$ is the $N+1$ electron valence wave function. The prime indicates that the valence wave function is calculated in the presence of the core potential. We can rewrite the Hamiltonian as

$$H = |G_0\rangle H_i \langle G_0| + \sum_g |G'_g\rangle H_f^g \langle G'_g|, \tag{9}$$

where

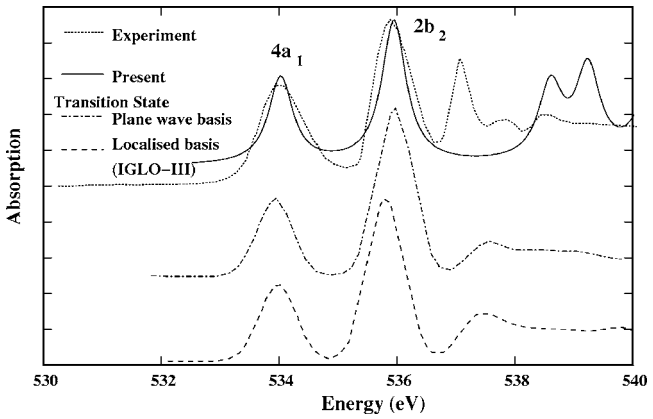

FIG. 1. Oxygen K-edge XANES of water. Calculations are performed at the HF level using the 6-311++G** basis. Excited states are calculated within TDHF. Also shown are experimental and computed spectra from Ref. 15. The line width $\Gamma=0.5$ eV.

$$H_i = \sum_{g'}^{\text{core}} \epsilon_{g'} \sum_{lm}^{\text{val}} \epsilon_{lm} c_l^\dagger c_m + \sum_{jklm}^{\text{val}} V_{jklm} c_j^\dagger c_k^\dagger c_m c_l, \tag{10}$$

$$H_f^g = \sum_{g'\neq g}^{\text{core}} \epsilon_{g'} \sum_{lm}^{\text{val}} [\epsilon_{lm} + U_{lm,g}] c_l^\dagger c_m + \sum_{jklm}^{\text{val}} V_{jklm} c_j^\dagger c_k^\dagger c_m c_l. \tag{11}$$

The absorption cross section finally becomes

$$\sigma_{\text{abs}}(\omega) = \frac{4\pi}{3\omega c}\sum_f \sum_{g,lm}\sum_\lambda \mu^\lambda_{lg}\mu^\lambda_{gm} \times \frac{\langle \Phi_i^N c_l|\Phi'^{N+1}_f\rangle\langle \Phi'^{N+1}_f|c_m^\dagger \Phi_i^N\rangle \Gamma}{(\omega + E_i - E_f)^2 + \Gamma^2}, \tag{12}$$

where Γ is a broadening due, e.g., to the finite core hole lifetime.

XANES calculations requires three ingredients: the dipole matrix elements, the many-body overlap factor, and the resonant energies. These were calculated using the method developed in Ref. 6.

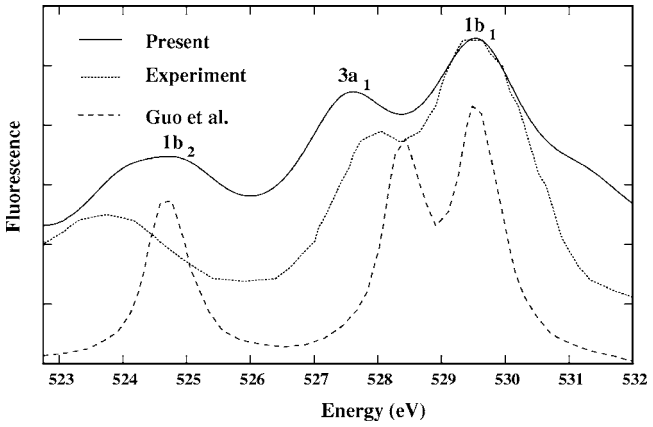

FIG. 2. Oxygen K-fluorescence spectra of water. Electronic structure calculations are performed using HF with the D95V+* basis set. Excited states are computed within TDHF. The x-ray excitation energy is 543 eV. $\Gamma=2.0$ eV. Also shown are experimental and computed spectra from Ref. 21.

B. Fluorescence

Computing resonant fluorescence spectra requires three states: the initial $|\Psi_i\rangle$, intermediate $|\Psi_e\rangle$, and final states $|\Psi_f\rangle$ with corresponding energies E_i, E_e, and E_f. We shall factorize the valence and core wave functions of the deep-core Hamiltonian [Eq. (1)] as

$$|\Psi_i\rangle = |\Phi_\nu^N\rangle|G_0\rangle, |\Psi_e\rangle = |\Phi_{\nu'}'^{N+1}\rangle|G_g'\rangle, |\Psi_f\rangle = |\Phi_{\nu''}^N\rangle|G_0\rangle. \tag{13}$$

The effective Hamiltonian for $|\Psi_i\rangle$ and $|\Psi_f\rangle$ is given by Eq. (10), and $|\Psi_e\rangle$ is an eigenstate of Eq. (11). The fluorescence spectrum (ω_L is the excitation frequency; ω_S is the emitted photon frequency) is[19]

$$S(\omega_L,\omega_S) = \sum_{i,f} P(i) \left| \sum_e \frac{\langle\Psi_f|\mu^\lambda|\Psi_e\rangle\langle\Psi_e|\mu^\lambda|\Psi_i\rangle}{E_i - E_e + \omega_L + i\Gamma} \right|^2 \times \delta(E_i - E_f + \omega_L - \omega_S), \tag{14}$$

where $P(i)$ is the equilibrium population of the initial state and Γ is the inverse lifetime of $|\Psi_e\rangle$. Upon substitution of Eq. (6) and Eq. (13) into Eq. (14), we obtain

$$S(\omega_L,\omega_S) = \sum_{\nu''} \left| \sum_{\nu'} \sum_{g,lm} \sum_\lambda \mu_{lg}^\lambda \mu_{gm}^\lambda \frac{\langle\Phi_{\nu''}^N c_l|\Phi_{\nu'}'^{N+1}\rangle\langle\Phi_{\nu'}'^{N+1}|c_m^\dagger\Phi_\nu^N\rangle}{E_\nu - E_{\nu'} + \omega_L + i\Gamma} \right|^2 \times \delta(E_\nu - E_{\nu''} + \omega_L - \omega_S), \tag{15}$$

where ν denotes either the ground electronic state or an optically excited state. The ν' (ν'') sum runs over all intermediate (final) states.

Electronic structure calculations were performed using GAUSSIAN 03. For XANES, the first 15 excited states of the core filled ground state and the first 50 excited states of the lowest core excited state were calculated using TDDFT and TDHF. The first 50 excited states of the core filled ground state and lowest core excited state were used in the fluorescence calculations.

III. RESULTS

Cavalleri and co-workers have studied the XANES spectra of water in gas phase, liquid water, and ice[14,15] within the TP formalism. They have analyzed the preedge feature of liquid water and ice in terms of the effect of breaking and forming of hydrogen bonds. In a recent work Cavalleri *et al.*[20] have demonstrated that theoretical modeling with DFT half core hole (HCH) potential on XANES of liquid water, ice, and water in gas phase gives a better agreement with the experiment than does that with DFT full core hole (FCH) potential. Guo *et al.*[21] have worked out the x-ray fluorescence spectra of water in gas phase as well as in liquid phase, employing the group theoretical approach. They studied the influence on the local electronic structure due to hydrogen bonds formed by surrounding water molecules. Odelius *et al.*[22] have studied the effect of vibrational excitations in the fluorescence spectra of water. Carniato *et al.*[16] have used their full core hole-lowest unoccupied molecular orbital (FCH-LUMO) approach and TP formalism to study the N *K*-edge XANES spectra of benzonitrile molecule in gas phase. They have also analyzed the vibrational profiles using a combined transition state theory and linear coupling model. Kashtanov *et al.*[23] have investigated the effect of hydrogen bond on the O *K* x-ray fluorescence spectra of liquid methanol. We have computed the XANES and fluorescence spectra of these molecules in the ground state and in optically excited states.

A. Water

HF calculations are performed using the 6-311++G** basis set (6-311 basis with double diffuse and polarization functions). Excited states are calculated using TDHF. Figure 1 compares the calculated XANES spectrum with the computed and experimental spectra from Ref. 15. The lowest peak (534.0 eV) corresponds to the transition from the orbital $1a_1$ to $4a_1$ (core to LUMO). The second peak (535.9 eV) corresponds to the transition from the orbital $1a_1$ to $2b_2$ (core to LUMO+1). We find a peak splitting of 1.92 eV, in close agreement with the experiment (1.90 eV).[15] Cavalleri *et al.*[15] used the transition potential method with localized and plane wave basis sets and obtained 183 and 2.04 eV, respectively. In a recent study Cavalleri *et al.*[20] have demonstrated that the DFT (FCH) method does not give Rydberg transitions in agreement with the experiment, whereas DFT (HCH) does. In our calculation we found that two lowest transitions in the XANES of water give a good agreement with the experiment, but not the Rydberg transitions. In the $Z+1$ approximation (which is analogous to the DFT (FCH) method), the oxygen atom is replaced by more electronegative fluorine atom. The induced charge transfer from neighboring atoms increases the population of p orbitals of fluorine and consequently screens the higher states. This may result in the large energy gap between $2b_2$ and Rydberg states.

The fluorescence spectrum [with excitation energy ω_L =543 eV (Ref. 21)] is shown in Fig. 2. The electronic configuration of water is $1a_1^2, 2a_1^2, 1b_2^2, 3a_1^2, 1b_1^2$. Ground state calculations are performed at the HF level with the D95V +* basis (Dunning/Huzinaga valence double-zeta function

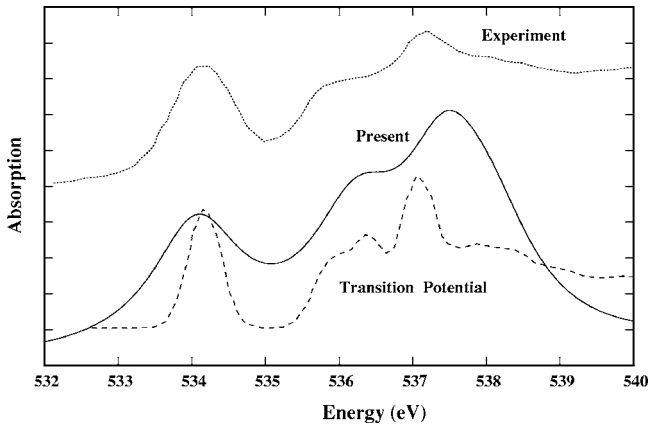

FIG. 3. Oxygen *K*-edge XANES of methanol molecule. A B3LYP calculation with the 6-311G** basis has been performed. Excited states are calculated within TDDFT. $\Gamma=1.5$ eV. Also shown are the experimental and computed spectra taken from Ref. 14.

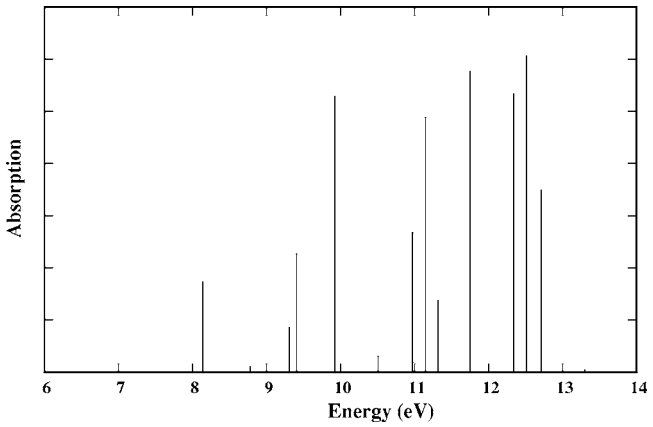

FIG. 4. Optical spectrum of methanol. TDDFT with the 6-311G** basis was employed.

with a single set of diffuse functions and a set of polarization functions). TDHF was used to calculate 50 excited states of the initial and intermediate states. The spectrum is dominated by transitions from three highest occupied molecular orbitals $1b_1$, $3a_1$, and $1b_2$, (oxygen $2p$) to the $1a_1$ orbital (oxygen $1S$). Also shown is the experimental spectrum and calculated spectrum by Guo *et al.*[21] Our peak intensities are in good agreement with the experiment. In the computed spectrum, peaks corresponding to $1b_1 \rightarrow 1a_1$ and $3a_1 \rightarrow 1a_1$ transitions are blue shifted by ~3 eV, and the lowest peak corresponding to the $1b_2 \rightarrow 1a_1$ transition is blue shifted by ~4 eV compared to the experiment. For a better comparison, we have rescaled the experimental and calculated spectra taken from Ref. 21. Peaks $1b_2 \rightarrow 1a_1$ and $3a_1 \rightarrow 1a_1$ are in close agreement with the experiment. Peak $1b_2 \rightarrow 1a_1$ is blue shifted by ~1 eV compared to the experiment. This is due to the neglect of vibrational effects in the calculation. In a recent work Odelius *et al.*[22] have shown that the fluorescence spectrum of gas phase water can be described correctly if vibrational excitations are included.

B. Methanol

The simulated oxygen *K*-edge XANES of methanol is shown in Fig. 3 and compared with the experiment and with earlier TP computations.[14] Ground state calculations were performed within B3LYP using the 6-311G** basis. Excited states are computed using TDDFT. The lowest peak at 534.0 eV is due to the transition from $1s$ to $2p$ atomic orbital of oxygen [LUMO (π^*)]. The second (536.2 eV) peak is due to the transition from the core to either LUMO or LUMO +1 with mostly a p character of oxygen. However, LUMO +1 of $|\Phi_0^N\rangle$ gives a maximum overlap with the LUMO of $|\Phi_0'^{N+1}\rangle$. Similarly the transitions at 537.5 eV is described by the excitation from orbital 10 [highest occupied molecular orbital (HOMO) of $|\Phi_0'^{N+1}\rangle$] to carbon located orbital 12 (LUMO+1 of $|\Phi_0'^{N+1}\rangle$), corresponding to orbitals 13 and 14 of $|\Phi_0^N\rangle$. The fourth dominant transition (538.1 eV) is described by the excitation from orbital 10 to orbital 14 of $|\Phi_0'^{N+1}\rangle$, corresponding to orbital 13 of $|\Phi_0^N\rangle$.

TDDFT with the 6-311G** basis was employed to calculate the optical spectrum depicted in Fig. 4. We used one of the strongest transition from HOMO−3 (molecular orbital 6) to LUMO at 11.75 eV and another relatively weaker at 11.32 eV in the optical spectrum to compute the excited state XANES. The XANES spectrum of the optically excited state, from HOMO−3 to LUMO of $|\Phi_0^N\rangle$ with excitation energy of 11.75 eV, is shown in Fig. 5 (dot-dashed line). Also shown are the XANES of excited state, from HOMO−2 to LUMO of $|\Phi_0^N\rangle$ with excitation energy of 11.32 eV (dashed line) and that of the ground state (solid line). More transitions show up in the excited state XANES spectrum. The peaks are red shifted compared to the ground state spectrum. This is because when an electron is removed from the inner valence orbital in the optical excitation, the electrons occupying the outer valence orbitals respond to the optical hole. This is evident from the fact that the excited state XANES HOMO−3 to LUMO (dot-dashed) is more red shifted than HOMO−2 to LUMO) (dashed).

The 522.3 eV peak (dot-dashed) is due to the transition from the core to orbital 6 of $|\Phi_0^N\rangle$, where the photoelectron occupies the optical hole created (corresponding to the

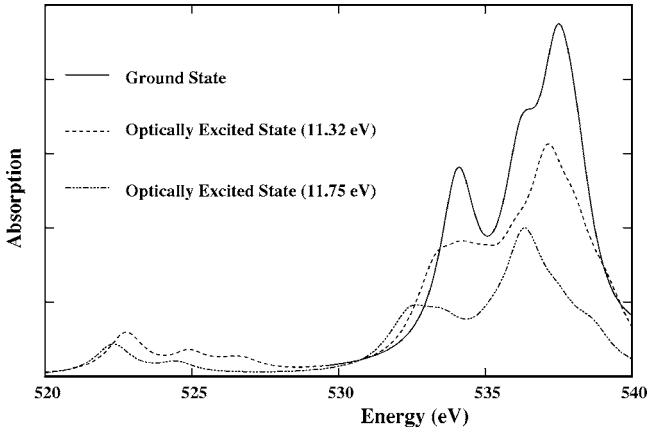

FIG. 5. Oxygen *K*-edge XANES of methanol. The solid line is the ground state and the dashed line is the optically excited state from HOMO−2 (molecular orbital 7) to LUMO of $|\Phi_0^N\rangle$ with excitation energy of 11.32 eV. The dot-dashed line is the optically excited state from HOMO−3 (molecular orbital 6) to LUMO of $|\Phi_0^N\rangle$ (one of the strongest transitions in the optical spectrum). $\Gamma=1.5$ eV.

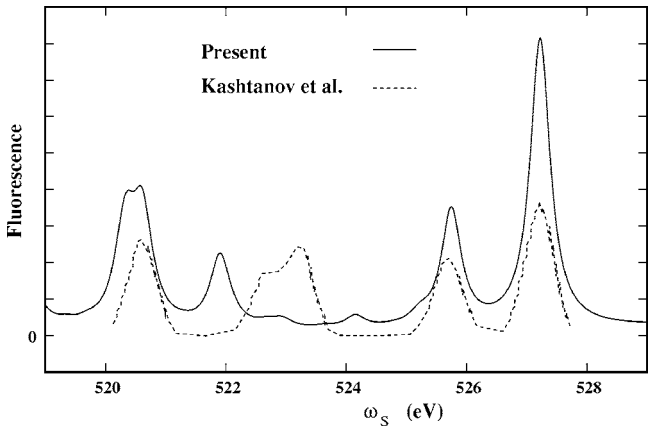

FIG. 6. Oxygen K-fluorescence spectra of methanol. Ground state calculations are performed using HF with the D95V basis set. Excited states are computed within TDHF. The x-ray excitation energy is 536.7 eV. $\Gamma=0.4$ eV. Also shown is the computed spectrum from Ref. 23.

ground state of $|\Phi_0'^{N+1}\rangle$). The other weak peak at 524.5 eV is also due to the transition from the core to orbital 6 of $|\Phi_0^N\rangle$ (corresponding to $|\Phi_1'^{N+1}\rangle$). The rest of the spectrum is dominated by four strongest transitions corresponding to the final states 10, 15, 29, and 33 at 532.4, 533.6, 536.3, and 537.5 eV, respectively. Transitions corresponding to the final states 12, 26, 32, and 44 at 533.1, 535.3, 536.7, and 538.6, respectively, are also seen. The final states 10 and 12 in the excited state XANES at 532.4 and 533.1 eV give a maximum overlap with orbitals 11 and 14 of the initial state, respectively. Similarly, the final states 1 and 2 at 536.2 and 537.5 eV in the ground state XANES have a maximum overlap with the orbitals 11 and 13, 14 of the initial state, respectively.

The oxygen K-fluorescence spectrum (the x-ray excitation energy is $\omega_L=536.7$ eV) is shown in Fig. 6 and compared with the computed spectrum at the HF level using the Sadlej basis by Kashtanov *et al.*[23] The optical spectrum is shown in Fig. 7. Ground state calculations are performed at the HF level with the D95V basis. Excited states are calculated using TDHF. We find an agreement of our computed spectrum with the experiment.[24] Five dominant transitions at 527.0, 525.5, 521.7, 520.4, and 520.1 eV are seen. The computed fluorescence spectra of optically excited states

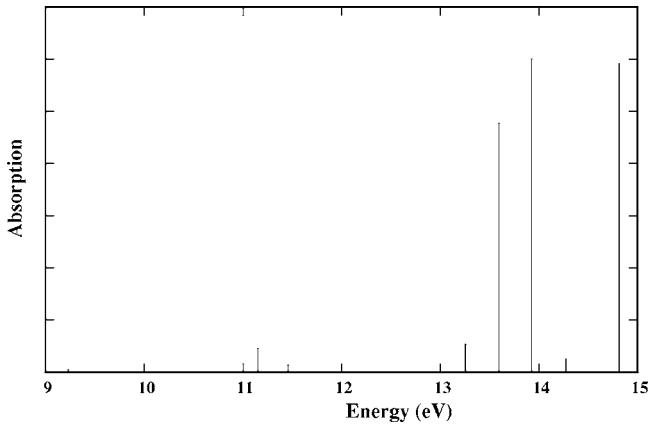

FIG. 7. Optical spectrum of methanol calculated with TDHF and the D95V basis.

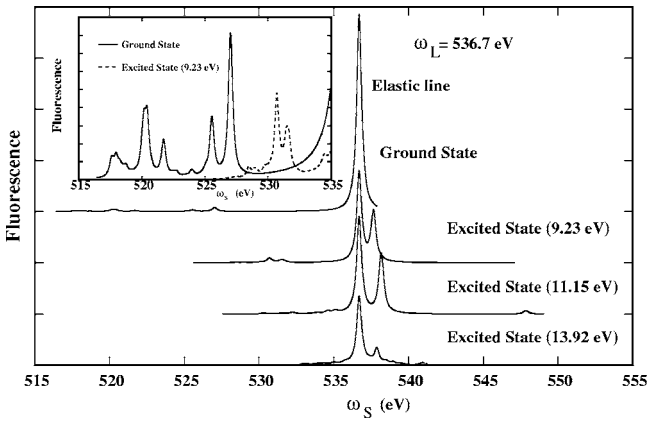

FIG. 8. Oxygen K-fluorescence spectra of methanol in the ground state and lowest excited states. Ground state calculations are performed within HF using the D95V basis set. Excited state calculations are performed within TDHF. The x-ray excitation energy is 536.7 eV. The inset shows a zoomed spectrum of the excited state (9.23 eV) along with that of the ground state. $\Gamma=0.4$ eV.

with excitation energies 9.23 (HOMO to LUMO), 11.15 (HOMO−1 to LUMO), and 13.92 eV (HOMO−2 to LUMO) are shown in Fig. 8 along with the ground state spectrum. In the inset we show the excited state (9.23 eV) spectrum on an expanded scale along with the ground state. The excited state spectra are blue shifted. Additional peaks appear in the excited state fluorescence with energies larger than the elastic peak. These correspond to the recombination of an optically excited electron with the core hole.

C. Benzonitrile

Figure 9 compares the simulated N K-edge XANES spectrum of benzonitrile with experimental and computed (TP) spectra.[16] Ground state calculations have been performed using (a) B3LYP and (b) HF. The D95** basis (Dunning/Huzinaga full double zeta function with double polarization function) set has been used in both the calculations. Excited states are computed using (a) TDDFT and (b) TDHF. There are 27 occupied orbitals in the core filled ground state. The first of the two strongest peaks at 398.8 eV is due to the transition from $1s$ core to $5p_z$ of nitrogen [π^* antibonding $(4b_1)$], i.e., from the core to molecular orbital 28 (LUMO). The other peak at 399.8 eV corresponds to the transition from $1s$ core to $5p_y$ of nitrogen [π^* antibonding $(10b_2)$]. This is molecular orbital 30 (LUMO+2). Notice from Fig. 9(a) that the B3LYP calculation gives an intensity ratio of the spectrum which is in good agreement with the experiment and a peak splitting of 0.73 eV (experiment, 1.0 eV). Figure 9(b) is for the HF calculation. The resulting spectrum gives a peak splitting of 1.0 eV which is in excellent agreement with the experiment. However, the intensity ratio is different from the experiment. We have introduced ~0.75 eV blue edge shift in the spectrum of the DFT calculation [Fig. 9(a)] and ~1 eV in the HF calculation [Fig. 9(b)] for a better comparison with experiment.

The optical spectrum of benzonitrile is shown in Fig. 10, computed within TDDFT (left) and TDHF (right) using the D95** basis. From the TDDFT calculation, we selected two strong optical transitions at 5.58 eV (HOMO to LUMO) and

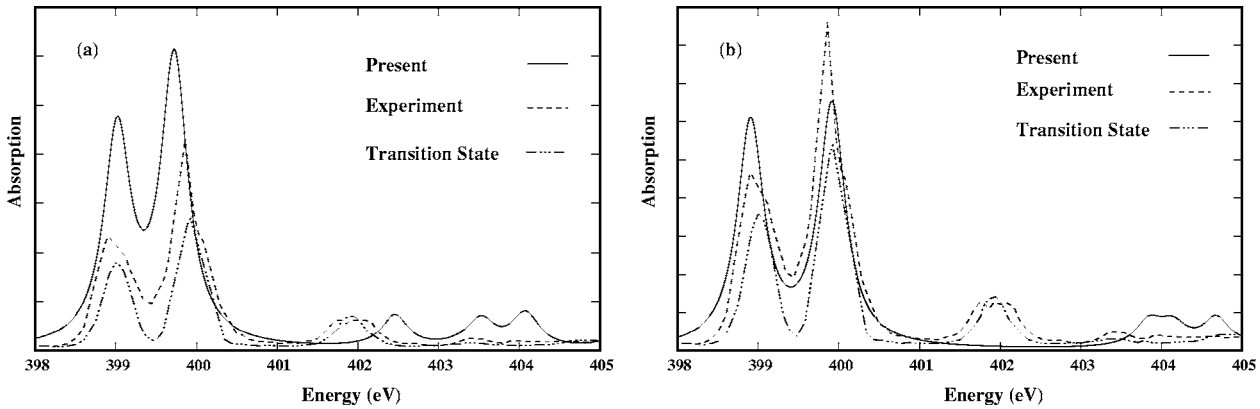

FIG. 9. Nitrogen *K*-edge XANES of benzonitrile. (a) Ground state calculations are performed using B3LYP with the D95** basis set. Excited states are calculated using TDDFT. The peak splitting is 0.73 eV (b) Ground state calculations are performed using HF with the D95** basis set. Excited states are calculated using TDHF. The peak splitting is 1.0 eV. $\Gamma=0.4$ eV.

7.39 eV (HOMO−3 to LUMO) to study the optically excited XANES. From the TDHF calculation we select one transition at 5.62 eV (HOMO to LUMO). We show the XANES spectra of an optically excited state in Fig. 11. Ground state calculations are performed within B3LYP using the D95** basis. Excited states are computed using TDDFT. The upper plot is the ground state. The middle plot is the excited state corresponding to the HOMO to LUMO transition (5.58 eV). The lower plot is the excited state corresponding to the HOMO−3 to LUMO transition (7.39 eV). Notice the preedge feature in the excited state spectra in both cases. The lower spectrum is more red shifted than the middle one, with respect to the ground state. Additional transitions appear in the excited state.

In the excited state spectrum (5.58 eV), the preedge peak at 392.6 eV is due to the transition from the core to molecular orbital 27, where an optical hole was created in the excitation. Another weak peak at 393.4 eV corresponds to the transition from the core to molecular orbital 30. Two strong transitions (396.1 and 396.9 eV) are from the core to orbital 31 (corresponding to final states 3 and 4). The strongest peak in the spectrum due to two closely spaced transitions at 397.7 and 397.8 eV is described by the excitations $26\rightarrow28$ and $26\rightarrow29$ of the $Z+1$ state, which give a maximum overlap with orbitals 28 and 30 of the initial state. The other two main transitions at 399.3 and 399.6 eV are described by the excitations $27\rightarrow30$, $23\rightarrow28$ and $26\rightarrow31$, $28\rightarrow34$ (corresponding to final states 16 and 20 of the $Z+1$ state).

In the excited state spectrum (7.39 eV), the first peak (390.8 eV) is due to the transition from the core to orbital 24 of $|\Phi_0^N\rangle$, where an optical hole was created. The 394.3 eV peak comes from the transition from the core to orbital 24 of $|\Phi_0^N\rangle$, corresponding to final state 3 ($|\Phi_3'^{N+1}\rangle$). The 395.1 eV peak is due to a transition from the core to orbital 31. One of the two strongest peaks in the spectrum is due to two closely spaced transitions at 395.9 and 396.0 eV from the core to orbital 28 and 30, respectively (final states 10 and 11 give a maximum overlap with orbitals 28 and 30 of the initial state). The other strongest peak at 398.2 eV can be described by the excitation $23\rightarrow28$ of the $Z+1$ state (final state 23), corresponding to orbital 28 of the initial state.

Even though the ground state XANES computed within both B3LYP and HF are similar, they predict different XANES from the lowest optical excited state. Figure 12 depicts XANES of the optically excited state (dashed line) from HOMO to LUMO (5.62 eV) along with that of the ground state (solid line). Ground state calculations are performed within HF using the D95** basis. Excited states are computed using TDHF. The preedge peak at 391.8 eV is due to the transition from the core orbital to orbital 27 (HOMO of $|\Phi_0^N\rangle$), where an optical hole was created (corresponding

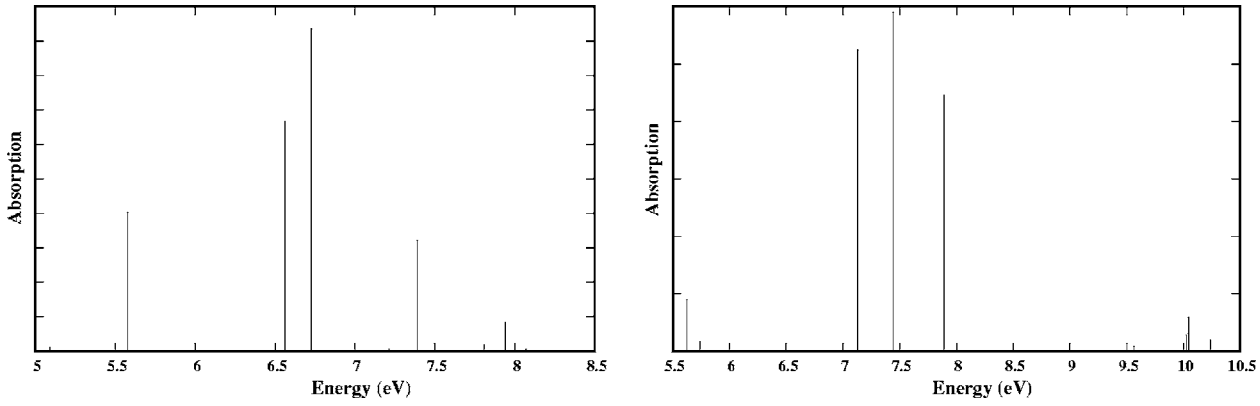

FIG. 10. Optical absorption of benzonitrile calculated using TDDFT (left) and TDHF (right). The D95** basis set was employed in both calculations.

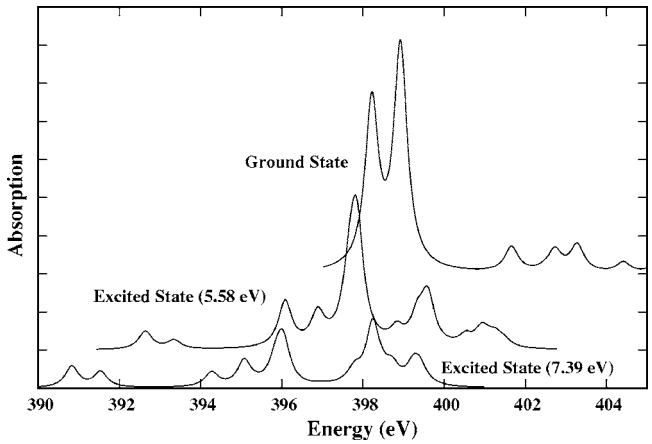

FIG. 11. Nitrogen *K*-edge XANES of benzonitrile. Ground state electronic structure calculations are performed using B3LYP with the D95** basis set. Excited states are computed using TDDFT. The upper trace is the ground state; middle and lower traces are the optically excited states from HOMO (molecular orbital 27) to LUMO (molecular orbital 28) with excitation energy of 5.58 eV and from HOMO−3 (molecular orbital 24) to LUMO with excitation energy of 7.39 eV, respectively. $\Gamma=0.4$ eV.

to the ground state of $|\Phi_0'^{N+1}\rangle$). Two closely spaced transitions at 396.9 and 397 eV corresponding to final states 3 and 4 are given by the excitations $28\rightarrow31$ and $\rightarrow29$ of $|\Phi_0'^{N+1}\rangle$, which give a maximum overlap with orbitals 27, 32 and 32 of $|\Phi_0^N\rangle$, respectively. Another significant transition at 398.4 eV is described by final state 8 corresponding to the excitation from orbital $26\rightarrow28$ of $|\Phi_0'^{N+1}\rangle$, which gives a good overlap with orbital 32 of $|\Phi_0^N\rangle$. The excited state spectrum is slightly red shifted compared to the ground state. There is an increase in the splitting of two strongest peaks and a change in the intensity ratio in the excited state.

D. H_2S

The optical spectrum of H_2S is shown in Fig. 13. We have used TDHF with the 6-311++G** basis. Three strong optical transitions are selected for the excited state XANES

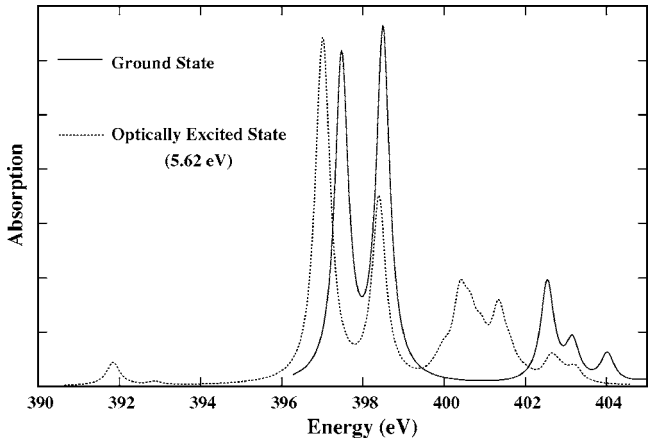

FIG. 12. Nitrogen *K*-edge XANES of benzonitrile molecule. Ground state electronic structure calculations are performed using HF with the D95** basis set. The solid (dashed) line is the ground state (optically excited state from HOMO to LUMO with excitation energy of 5.62 eV). $\Gamma=0.4$ eV.

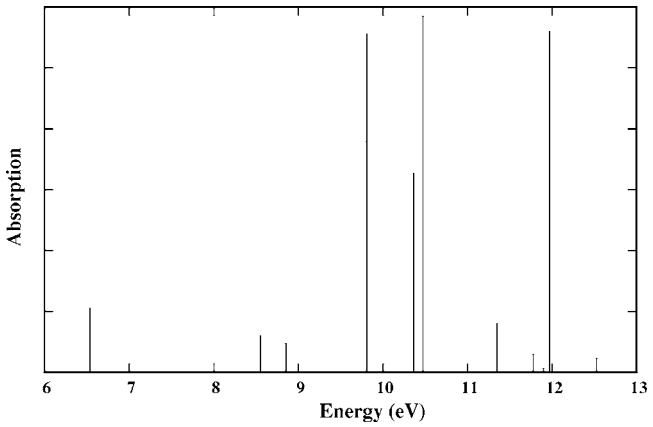

FIG. 13. Optical spectrum of H_2S calculated using TDHF with the 6-311++G** basis.

computation: 6.54 eV (HOMO to LUMO), 9.80 eV (HOMO−1 to LUMO), and one of the strongest transitions at 11.97 eV (HOMO−2 to LUMO).

Figure 14 shows the simulated sulphur *K*-edge XANES of hydrogen sulphide. From top to bottom we show the ground state XANES, optically excited state from HOMO to LUMO with excitation energy of 6.54 eV, the excited state from HOMO−1 to LUMO with excitation energy of 9.80 eV, and the excited state from HOMO−2 to LUMO with excitation energy of 11.97 eV. Ground state calculations are performed at the HF level using the 6-311++G** basis. Excited states are computed within TDHF. The ground state XANES gives a good agreement with the experimental spectrum of Mayer *et al.*[25] There are three main peaks. The first at 2472.5 eV is due to the transition from the core to the LUMO (orbital 10). Two closely spaced transitions at 2475.99 and 2476.04 eV are due to the transitions from the core to orbitals 12 and 13, respectively. The third peak is described by a transition from the core to either orbital 14 or orbital 16.

As expected, in the excited state XANES (6.54 eV) there

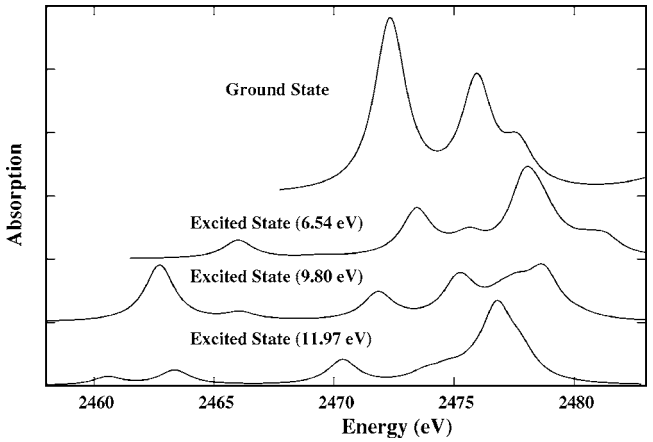

FIG. 14. S *K*-edge XANES of H_2S. Ground state calculations are performed using HF with the 6-311++G** basis. Excited states are calculated using TDHF. The top trace is the ground state; the middle two are the optically excited states from HOMO (molecular orbital 9) to LUMO with excitation energy of 6.54 eV and from HOMO−1 to LUMO with excitation energy of 9.80 eV. The bottom trace is the optically excited state from HOMO−2 to LUMO with excitation energy of 11.97 eV. $\Gamma=1.5$ eV.

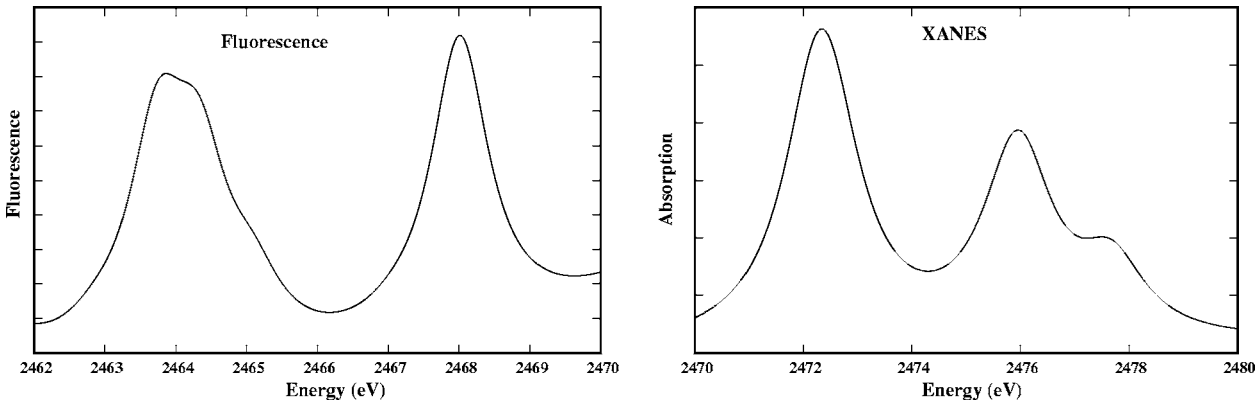

FIG. 15. S *K*-edge fluorescence and XANES of H_2S. Ground state calculations are performed using HF with the 6-311++G^{**} basis. Excited states are calculated using TDHF. For XANES $\Gamma=1.5$ eV and for fluorescence $\Gamma=1.0$ eV.

is a preedge peak at 2466.0 eV given by the transition from the core to the HOMO of $|\Phi_0^N\rangle$, where a hole was created optically. Additional transitions show up in the excited state. However, most transitions are the same as in the ground state XANES, except that the spectrum is blue shifted. This is to be expected, since an optical excitation from the HOMO to LUMO increases the positive charge on the absorbing atom. Therefore more energy is required to excite the core electron. The other two excited state spectra (excitation energies 9.80 and 11.97 eV) are red shifted compared to the ground state spectra. This is because when an electron is removed from the inner valence orbital in the optical excitation, the electrons occupying the outer valence orbitals respond to the created hole. The excited state XANES with excitation energy of 11.97 eV (HOMO−2 to LUMO) is more red shifted than the one with excitation energy of 9.80 eV (HOMO−1 to LUMO). New transitions, for instance, a new preedge peak appears in the excited states. Also the peak intensities change in the excited states.

The fluorescence spectrum of the S *K*-edge of H_2S is shown in Fig. 15 (left panel) for excitation energy of 2472.1 eV. Also shown is the ground state XANES spectrum (right panel). The three dominant transitions are from orbitals 9 (HOMO), 8 (HOMO−1), and 7 (HOMO−2) to the core

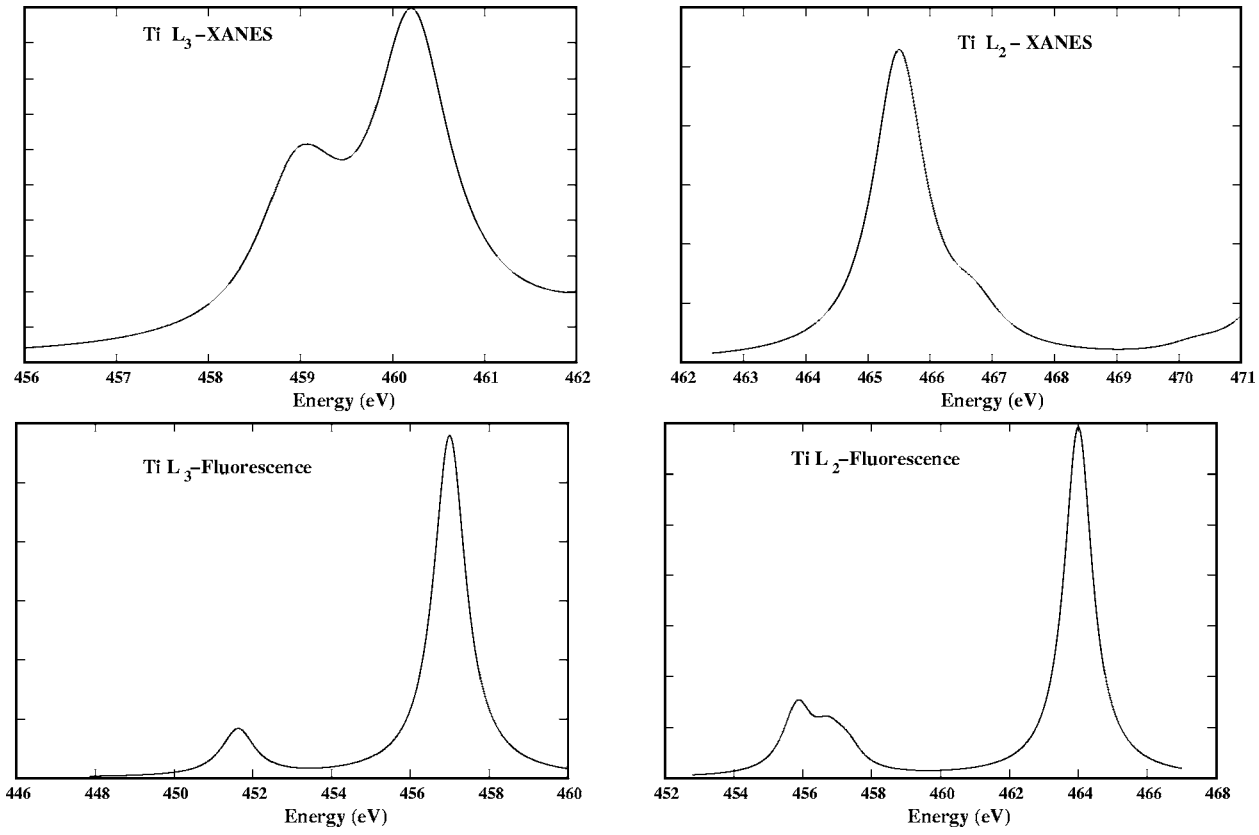

FIG. 16. Left column: titanium L_3-edge XANES (top) and fluorescence (bottom); right column: titanium L_2-edge XANES (top) and fluorescence (bottom) of $TiCl_4$. For L_3-edge (L_2-edge) edge XANES, ground state calculations are performed within HF using the 6-311G^{**} (6-311++G^{**}) basis. For L_3 (L_2) fluorescence, ground state calculations are performed within B3LYP (HF) using the 3-21G^{*} (6-311+G^{*}) basis. The excitation energy used for L_3 (L_2) is 457 (464) eV. $\Gamma=1.0$ eV.

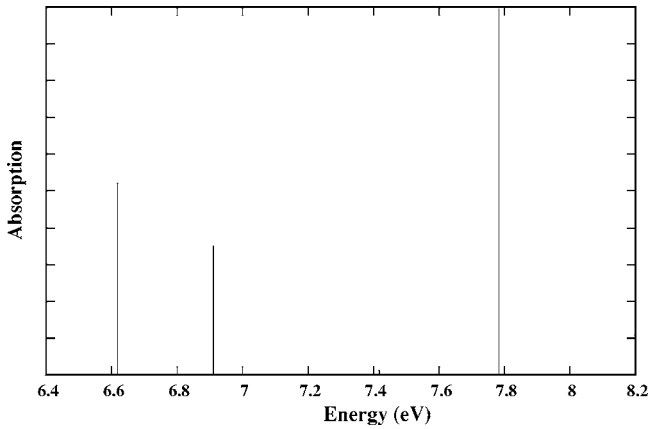

FIG. 17. Optical spectrum of $TiCl_4$ (TDHF with the 6-311++G^{**} basis).

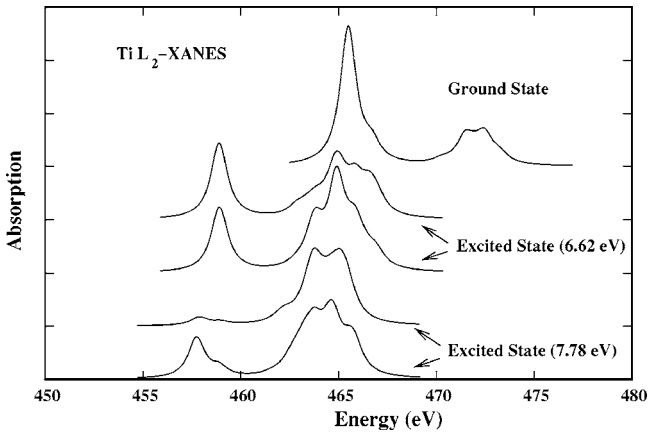

FIG. 18. Ti L_2-edge XANES of $TiCl_4$. The top trace is the ground state. The second and third from the top and the fourth and fifth from top are the excited states with excitation energies of 6.62 and 7.78 eV, respectively. Ground state calculations are performed within HF using the 6-311++G^{**} basis. Excited states are computed using TDHF. $\Gamma = 1.0$ eV.

orbital. These transitions are labeled $2b_1 \rightarrow 1a_1$, $5a_1 \rightarrow 1a_1$, and $2b_2 \rightarrow 1a_1$ in the experimental paper of Mayer *et al.*[25]

E. $TiCl_4$

Titanium L_3- and L_2-edge XANES spectra of $TiCl_4$ are shown in Fig. 16 (top two). For the L_3- and L_2-edge XANES computation, ground state electronic structure calculations were performed at the HF level using the 6-311G^{**} and 6-311++G^{**} basis sets, respectively. Excited states are computed within TDHF. We reproduced the experimental spectra of Hague and Tronc *et al.*[26] Almost all the strong transitions result from molecular orbitals 2 and 3 (L_2 edge) and orbitals 3, 4, and 5 (L_3 edge), which have the *p* character of titanium, are strongly mixed with *s* and *p* atomic orbitals of chlorine, and are centered around chlorine atoms, to the molecular orbitals 46, 48, 49, and 50, which have the strong *d* character of titanium. The computed fluorescence spectra shown in Fig. 16 (bottom two panels) are in close agreement with the experiment of Hague and Tronc *et al.*

We have simulated Ti L_2-edge excited state XANES. The optical spectrum of $TiCl_4$ is shown in Fig. 17. The TDHF calculation with 6-311++G^{**} was performed. There are three degenerate transitions at 6.62 eV. We pick two of them for excited state XANES calculations. In one of the electronic transitions, the HOMO−2 (orbital 43) to LUMO (orbital 46) transition gives the largest contribution. In the other electronic transition, the HOMO−1 to LUMO transition gives the largest contribution. Similarly, there are three degenerate transitions at 7.78 eV. We consider two of them. In one, the HOMO−4 to LUMO transition gives the largest contribution in the electronic transition. In the other, the HOMO−5 to LUMO transition gives the largest contribution. Figure 18 depicts the Ti L_2-edge XANES of $TiCl_4$. Topmost is the ground state. Second and third from the top and fourth and fifth from the top are excited states with excitation energies of 6.62 and 7.78 eV, respectively. Ground state HF calculations are performed with the 6-311++G^{**} basis. Excited states are computed using TDHF. The preedge peak in all spectra appears because of the transition from the core to the orbital with an optical hole. The second and third spectra (6.62 eV) from the top give identical XANES transitions. Similarly, the bottom two spectra (7.78 eV) give identical XANES transitions. A change in transition intensities implies a change in the charge distribution of the molecule in the two electronically excited states with the same excitation energy.

IV. CONCLUSIONS

Sum over states (SOS) calculations were carried out for the XANES and fluorescence spectra of molecules in their ground states and optically excited states. These calculations may be used to simulate optical pump x-ray probe experiments, whereby an optical pump excites the valence electrons which are then monitored by the x-ray probe. Ultrafast x-ray sources can provide attosecond snapshots of interatomic distances and changes in the geometry and charge distribution of molecules. Dynamical processes such as vibrational excitation, bond formation and breaking, geometry relaxation, and time-dependent solvation processes can be monitored on the fly. Molecular dynamics (MD) techniques can be employed for calculating the time resolved spectra of the photoexcited molecules. It will be interesting to perform a simulation on infrared pump x-ray probe in which an infrared pump excites a nuclear wave packet by selectively populating the vibrational levels in the ground electronic state and an x-ray probe detects the nuclear dynamics.

ACKNOWLEDGMENT

We gratefully acknowledge the support from the Chemical Sciences, Geosciences, and Biosciences Division, Office of Basic Energy Sciences, Office of Science, U.S. Department of Energy.

[1] J. Stöhr, *NEXAFS Spectroscopy* (Springer, New York, 1996).
[2] H. Ågren and F. Gel'Mukhanov, and C. Liegener, Int. J. Quantum Chem. **63**, 313 (1997).
[3] F. Gel'Mukhanov and H. Ågren, Phys. Rep. **312**, 87 (1999).
[4] C. Bressler, M. Saes, M. Chergui, D. Grolimund, R. Abela, and P. Pattison, J. Chem. Phys. **116**, 2955 (2002).
[5] C. Bressler and M. Chergui, Chem. Rev. (Washington, D.C.) **104**, 1781 (2004).
[6] L. Campbell and S. Mukamel, J. Chem. Phys. **121**, 12323 (2004) and references therein.
[7] S. Tanaka, V. Chernyak, and S. Mukamel, Phys. Rev. A **63**, 063405

(2001).
[8] S. Tanaka and S. Mukamel, Phys. Rev. A **64**, 032503 (2001).
[9] S. Tanaka and S. Mukamel, J. Electron Spectrosc. Relat. Phenom. **136**, 185 (2004).
[10] S. Tanaka and Y. Kayanuma, Phys. Rev. B **71**, 024302 (2005).
[11] J. J. Rehr and R. C. Albers, Rev. Mod. Phys. **72**, 621 (2000).
[12] F. de Groot, Chem. Rev. (Washington, D.C.) **101**, 1779 (2001).
[13] L. Triguero and L. G. M. Pettersson, Phys. Rev. B **58**, 8097 (1998).
[14] M. Cavalleri, H. Ogasawara, L. G. M. Pettersson, and A. Nilsson, Chem. Phys. Lett. **364**, 363 (2002).
[15] M. Cavalleri, M. Odelius, A. Nilsson, and L. G. M. Pettersson, J. Chem. Phys. **121**, 10065 (2004).
[16] S. Carniato, V. Ilakovac, J.-J. Gallet, E. Kukk, and Y. Luo, Phys. Rev. A **71**, 022511 (2005).
[17] G. D. Mahan, Phys. Rev. B **25**, 5021 (1982).
[18] P. Nozieres and C. T. DeDominicis, Phys. Rev. **178**, 1097 (1969).
[19] S. Mukamel, *Principles of Nonlinear Optical Spectroscopy* (Oxford University Press, New York, 1995).
[20] M. Cavalleri, M. Odelius, D. Nordlund, A. Nilsson, and L. G. M. Pettersson, Phys. Chem. Chem. Phys. **7**, 2854 (2005), and references therein.
[21] J.-H. Guo, Y. Luo, A. Augustsson, J.-E. Rubensson, C. Sathe, H. Ågren, H. Siegbahn, and J. Nordgren, Phys. Rev. Lett. **89**, 137402 (2002).
[22] M. Odelius, H. Ogasawara, D. Nordlund *et al.*, Phys. Rev. Lett. **94**, 227401 (2005).
[23] S. Kashtanov, A. Augustson, J.-E. Rubensson, J. Nordgren, H. Ågren, J.-H. Guo, and Y. Luo, Phys. Rev. B **71**, 104205 (2005).
[24] J.-E. Rubensson, N. Wassdahl, R. Brammer, and J. Nordgren, J. Electron Spectrosc. Relat. Phenom. **47**, 131 (1988).
[25] R. Mayer, D. W. Lindle, S. H. Southworth, and P. L. Cowan, Phys. Rev. A **43**, 235 (1991).
[26] C. F. Hague M. Tronc, Y. Yanagida, A. Kotani, J. H. Guo, and C. Sathe, Phys. Rev. A **63**, 012511 (2000).